Temporal structures in shell models

Fridolin Okkels
Department of Optics and Fluid Dynamics, Risø National Laboratory and Centre for Chaos and Turbulence Studies, The Niels Bohr Institute, University of Copenhagen, Blegdamsvej 17, DK-2100, Copenhagen, Denmark
(Received 18 August 2000; revised manuscript received 5 January 2001; published 23 April 2001)

The intermittent dynamics of the turbulent Gledzer, Ohkitani, and Yamada shell-model is completely characterized by a single type of burstlike structure, which moves through the shells like a front. This temporal structure is described by the dynamics of the instantaneous configuration of the shell amplitudes, revealing an approximate chaotic attractor of the dynamics.

DOI: 10.1103/PhysRevE.63.056214 PACS number(s): 05.45.−a, 47.27.Eq, 47.27.Gs, 47.27.Ak

I. INTRODUCTION

One of the main goals in current turbulence research is to understand the effect of intermittency in turbulence. It has long been known that intermittency produces corrections to the classical Kolmogorov $-5/3$ scaling law, and to other moments of the energy spectrum in the inertial range [1,2]. Still, very little is known about the intense intermittent structures found in turbulent flows [3].

Over the last decade turbulent shell models have been studied intensively because of their simplicity, and the excellent agreement of their statistics in comparison with those of experimentally measured turbulence [4–9]. Among the large numbers and types of different shell models the present work is based on the successful standard GOY shell model named after Gledzer, Ohkitani, and Yamada [4,5]. In a way this model reproduces the statistics of real intermittent turbulence far better than expected from its simplicity, and therefore the choice of the GOY model to model turbulence will not be questioned here.

Accepting the good statistical properties of the model, a question arises: What mechanism generates the intermittent behavior of the model? Benzi *et al.* [10] used a closure approach to answer this question, but this paper will follow another approach: Shell models have usually been viewed as high-dimensional systems, and have therefore been described by their statistical properties. However, the total number of free variables is normally only around 40, and this makes it possible to view shell models as low-dimensional systems and to analyze them using a dynamical system approach. Recently temporal structures, naturally arising in shell models, were thoroughly studied [11,12] and the approach of this paper will be a dynamical-system analysis of the coherent temporal structures found in the GOY model. Because of the intense dynamics during the temporal structures, they will be called bursts. It should be stressed that the purpose of viewing the model as a low-dimensional dynamical system is only to reveal the nature of its intermittent dynamics and nothing else. In the following the analysis has no direct physical relevance, since it is used only to understand the dynamics of the GOY model better. Once the intermittency of the GOY model is fully understood, it may inspire a better understanding of real intermittency found in turbulence.

The paper is organized as follows: Section II gives a detailed description of the bursts of the standard GOY model. Section III shows that an approximate chaotic attractor of the model exists, expressed by the collective dynamics of the neighboring shells.

II. GOY MODEL

All shell models simulate the flow of energy through wave number space in fully developed turbulence. The models consist of a system of coupled ordinary differential equations, where the energy is injected into low wave numbers by a constant forcing term. The energy then cascades up to the high wave numbers by means of a coupling term, where it is dissipated away by a viscosity term.

A. Construction

In the GOY model wave-number space is divided into N separate shells with characteristic wave numbers $k_n = k_0 \lambda^n$ $(\lambda = 2)$ where $n = 1, \ldots, N$, and k_0 is a constant determining the smallest wave number in the model. Each shell is assigned a complex amplitude u_n which can be imagined as the velocity difference on a scale $l_n = 1/k_n$. By assuming a conservation of phase space, energy and helicity, and interactions among the nearest and next nearest neighbor shells, one can arrive at the following set of evolution equations [5,7,9]:

$$\left(\frac{d}{dt} + \nu k_n^2\right) u_n = i k_n \left(u_{n+1}^* u_{n+2}^* - \frac{\delta}{2} u_{n-1}^* u_{n+1}^* - \frac{1-\delta}{4} u_{n-2}^* u_{n-1}^* \right) + f \delta_{n,4}, \qquad (1)$$

with boundary conditions $u_{-1} = u_0 = u_{N+1} = u_{N+2} = 0$, and constant forcing f on the fourth shell.

Set (1) of N coupled ordinary differential equations is numerically integrated by standard techniques [12]. In the simulations, we use the following standard values $\delta = 1/2$, $N = 19$, $\nu = 10^{-6}$, $k_0 = 2^{-4}$, and $f = (1+i) \times 0.005$ as found in earlier work [8,6,7,9]. Since the present work is based on the standard GOY model, all the basic properties and characteristics of the model, such as time scales, transitions, etc., are found in the former references. As a result time will be measured in natural units (n.u.) arising directly from the integration of the model.

B. Conservation laws, fixed points, and invariance

The strength of the shell models relates to their simplicity of construction, which can be justified because they possess

the same conservation laws and invariants as the Naiver-Stokes equations, i.e., the basic equations governing fluid dynamics. As for other shell models, the GOY model exhibits these conservation laws in the absence of forcing and viscosity ($f=\nu=0$), reducing the right side of Eq. (1) to a coupling term.

The conservation of phase space is enforced as the coupling term does not contain u_n. The remaining conserved quantities are quadratic, i.e., they can be written in the form $Q_\alpha=\Sigma k_n^\alpha |u_n|^2$. Using the relation $\frac{1}{2}(\dot{u}_n^2)=u_n\dot{u}_n$, and inserting Q_α into the model, the coupling term becomes three terms of three successive amplitudes multiplied together. Comparing these three terms gives the following relation on α: $1-\delta 2^\alpha-(1-\delta)2^{2\alpha}=0$, with two solutions $\alpha=0$ and $\alpha=-\ln_\lambda(\delta-1)$. The first ($\alpha=0$) corresponds to the conservation of energy, and the other to helicity conservation in the case of three-dimensional turbulence ($\delta<1$) and to enstrophy conservation in the case of two-dimensional turbulence ($\delta>1$) [7,8,12].

The fact that the coupling term multiplied by u_n gives three terms, all similar within prefactors and displacements in indices, makes the dynamics of the model invariant to the following changes in the complex amplitude phase:

$$\left.\begin{aligned} u_n &\to e^{i\alpha}u_n \\ u_{n+1} &\to e^{i\beta-\alpha}u_{n+1} \\ u_{n+2} &\to e^{i(-\beta)}u_{n+2} \end{aligned}\right\} \quad \text{where } n \text{ modulus } 3=1, \qquad (2)$$

and α and β are free parameters [13]. This invariance affects not only the phases but also the full dynamics of the model, since every third shell tends to follow the same behavior [12].

Thinking of the GOY model as a dynamical system, a basic thing to study is the fixed points of the model: $\dot{u}_n=0$, $n=1\ldots N$. Again, requiring an inviscid and unforced model ($f=\nu=0$) gives two nontrivial scaling fixed points: $u_n=k_n^{-z}g(n)$, with $z=\frac{1}{3}$ and $\frac{1}{3}[1-\ln_\lambda(\delta-1)]$, where $g(n)$ is an arbitrary function of period 3 in n coming from the invariance of the model. The first fixed point $u_n\sim k_n^{-1/3}g(n)$ corresponds to the Kolmogorov $-\frac{5}{3}$ scaling law, and will be called the Kolmogorov fixed point; while the other solution results in an alternation of the amplitudes [8,12]. In spite of the simplicity of the the Kolmogorov fixed point, it plays a crucial role in the later analysis of the model.

III. DYNAMICS OF THE MODEL

At large time scales the dynamics of the model may seem stochastic, but as the time span is refined distinct spikes emerge, and in the end the dynamics is noiseless and fully resolved even during the most dramatic changes. To observe the general behavior we monitor $|u_n(t)|$ as a function of time, and due to large variations in magnitude it is shown by a semilogarithmic plot in Fig. 1. The higher shells have the smallest absolute value and the fastest variations while the lower shells have large absolute values and vary over a longer time span. Two main features stand out from Fig. 1: All the higher shells evolve in a synchronized manner, and

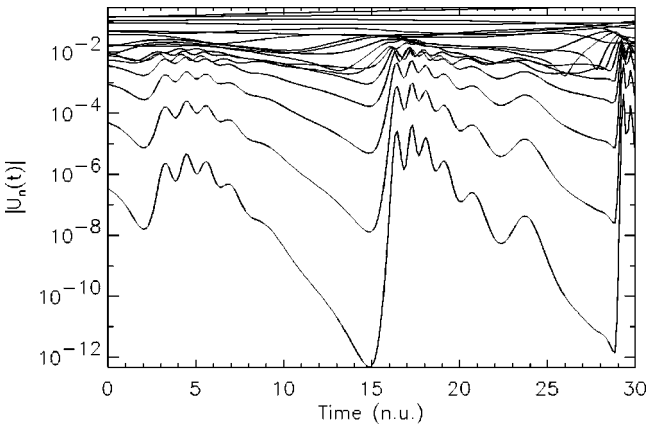

FIG. 1. A typical evolution of the norm of the amplitudes $|u_1|\ldots|u_{18}|$ in time of natural units.

the evolution follows a general pattern of strong bursts interchanged with oscillatory relaxation. During the evolution of the model, bursts occur randomly in time with great variations in their strength.

A. Organization of shell dynamics

The synchronization of the different shells is a result of the coupling between the shells, causing the model to self-organize into the types of behavior seen in Fig. 1. The organization in the model is shown most clearly by the local two-point complex correlation function, measuring how the dynamics of a given shell is correlated to its neighborhood of both shells and in time. It is defined, using the two shortcuts

$$U_0=U_{n_0}(t), \quad U_\Delta=U_{n_0+\Delta n}(t+\Delta t),$$

by

$$\Gamma(\Delta t,\Delta n)=C(U_0,U_\Delta)=\frac{\overline{U_0^*\cdot U_\Delta}-\overline{U_0^*}\cdot\overline{U_\Delta}}{\sqrt{(\overline{|U_0^2|}-\overline{|U_0|}^2)(\overline{|U_\Delta^2|}-\overline{|U_\Delta|}^2)}}, \qquad (3)$$

and where the averages are taken over time.

The information gained from $|\Gamma(\Delta t,\Delta n)|$ is divided into two parts: First, only the norm of the complex amplitudes is correlated, replacing U_0 and U_Δ by their norms. This is shown on the left side of Fig. 2 as a contour plot, where the dark area shows the strongest normalized correlation. Second the full complex amplitudes are correlated, and shown in the same manner on the right side of Fig. 2. Both correlations have $n_0=15$, and are averaged over 40.000 n.u., and correspond roughly to a time-span of approximately 4000 successive bursts.

The left plot shows that all the amplitudes in the model are strongly correlated from the forcing at the fourth shell up to the highest shells. This strong correlation is due to the organization of the amplitude dynamics during both bursts, and the succeeding strong oscillations. The same plot also shows the motion of the burst through the shells by the time shift of the correlation peaks for increasing Δn. When taking

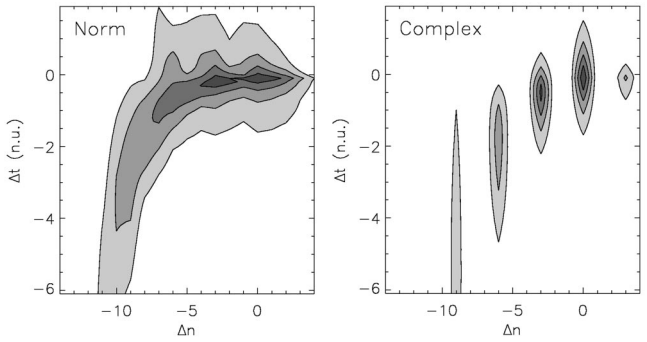

FIG. 2. The two-point correlation in shells and time of natural units, first for the norm of the amplitudes and second for the pure amplitudes, based at the 15th shell.

the amplitude phases into account, the correlation function changes radically, as seen on the right plot. Now only every third amplitude is correlated, as a result of the period-3 invariance of the model: From the invariance [Eq. (2)] it is always possible to change the phases of $u_{n+1}(t)$, $u_{n+2}(t)$ (n modulus $3=1$) by varying β, while keeping the dynamics of $u_n(t)$ fixed. As a result only correlations between every third complex amplitude can arise. It should be noted that the correlations of this section serve as pure data-series analysis, and should not be interpreted as a stochastic description of the model.

Figure 2 also shows how the characteristic time scale changes among the different shells. This is seen by the extent of the correlation peaks in time, which decreases with the shell number. When relating the characteristic time scale to the turnover time (τ_n), this dependence comes direct-from dimensional analysis [1].

B. Front motion during burst

The motion of bursts is a part of a more general motion of different organizations of the amplitudes traveling with exponentially increasing speed from the lower shells toward the higher shells, where they vanish because of viscosity [11]. A way to see this is to look at the changes in the instantaneous amplitude spectre during the motion of a burst. This is shown in Fig. 3 by snapshots of $\ln|u_n(t)|$ vs n, where the time between snapshots decreases by a factor of $1/\sqrt{2}$, giving roughly an equidistant motion of the burst. As for all other bursts Fig. 3 reveals that the burst travels through the shells as a front, keeping the same overall shape in the inertial subrange. Just at the maximum rise of the amplitudes, the overall scaling exponent of the inertial range is a bit lower than the Kolmogorov scaling law shown by the dashed line in Fig. 3. Immediately after the last snapshot, all the shells enter the oscillatory state.

C. Real-valued model

When decomposing the amplitudes in polar coordinates ($u_n=r_n e^{i\theta_n}$) the dynamics of the model depends critically on sums of three successive phases: $\theta_n+\theta_{n+1}+\theta_{n+2}$ [10,12]. It turns out that this sum stays very close to $-\phi$ for all shells participating in a burst, and as a consequence the effect of

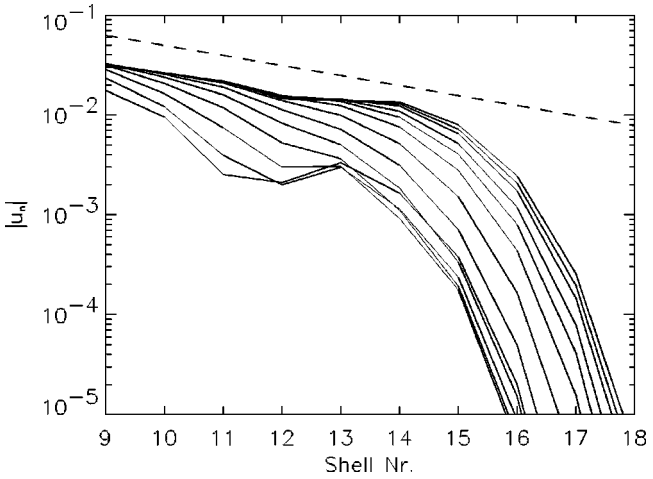

FIG. 3. Snapshots of $\log|u_n|$ during the *cascade* of a burst.

the complex phases vanishes during bursts [12]. This makes it possible to base the following analysis on a real-valued version of the GOY model, having real-valued amplitudes defined originally as $r_n=|u_n|$, with no conjugations and ''-1'' instead of ''i'' in front of the coupling term:

$$\left(\frac{d}{dt}+\nu k_n^2\right) r_n = -k_n\left(r_{n+1}r_{n+2}-\frac{1}{4}r_{n-1}r_{n+1}-\frac{1}{8}r_{n-2}r_{n-1}\right) + f\delta_{n,4}. \tag{4}$$

Although r_n in Eq. (4) originates from the polar decomposition of u_n, it will be both positive and negative during the dynamics of Eq. (4), but this is nothing but a discrete phase invariance since Eq. (2) still holds for Eq. (4) with α and β being whole multiples of π. To justify the real-valued model, Fig. 4 shows the evolution of Eq. (4) with r_n as a function of time to the left and $\log(|r_n|)$ as a function of time to the right. The only radical change caused by abandoning the complex phases of the standard GOY model is that the dynamics becomes periodic in time. However, this will be of no concern, since we will be concentrating on the dynamics during bursts. Note the similarity between the right side of Figs. 4 and 1, especially during bursts, which justifies the use of Eq. (4) in the following analysis.

To summarize this first part of this paper we have observed that the dynamics of the GOY-shell model is dominated by strong bursts moving up through the shells like a front, thus creating strong correlations (among the shells of

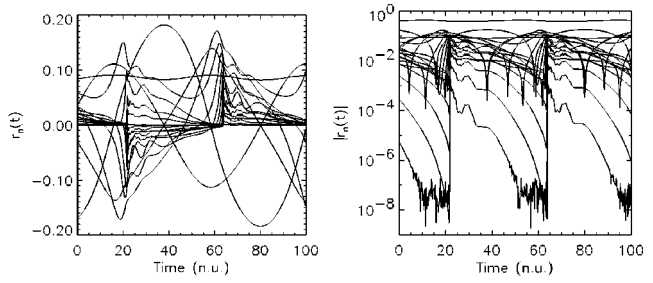

FIG. 4. The evolution of the real-valued GOY model.

the model). The next part of the paper will concentrate on the mechanism creating these bursts.

IV. LOCAL VARIABLES

Making an analogy to real turbulence, we have seen that bursts ''cascade'' nearly unaffected up through the shells like a front. If for the moment we assume these fronts to be unaffected during a cascade, then the coupling term for each shell will experience the same action from its neighboring shells as a burst passes through, and thus they will produce the same reaction on the dynamics of the corresponding shell participating in the burst. This indicates that a full understanding of bursts may be revealed by simply analyzing the behavior of a single generic coupling term during the passing of a burst.

To begin, we observe that the coupling term depends only on the instantaneous configuration of the neighboring shells, and has no explicit dependence on the present or past states. Then, if we restrict ourselves to the inertial range, neglecting forcing and viscosity, the neighboring shells may thus be seen as *a local phase space* of a shell, since their configuration through the coupling term exactly determines the instantaneous dynamics ($\dot{r}_n$) of the amplitude r_n. To characterize this local phase space, each set of neighboring shells will be called *local shells*, $\vec{L}_n=(r_{n-2},r_{n-1},r_{n+1},r_{n+2})$ of the nth shell, and should not be seen as a part of the other amplitudes but rather as an isolated set of variables determining $\dot{r}_n$.

The configuration of $\vec{L}_n$ will be described by first choosing the slope of $\ln_\lambda(\vec{L}_n)$, which is nothing but the local scaling exponent at the nth shell. To continue, we define

$$\vec{\eta}_n \equiv \ln_\lambda(\vec{L}_n), \tag{5}$$

and choose the mean, curvature, and third order component of $\vec{\eta}_n$. This gives the *local variables*. $\vec{P}_n=(A_n,B_n,C_n,D_n)$ of r_n, defined as the coefficients of the projection of $\vec{\eta}_n$ on the orthogonal basis given by the matrix **T**:

$$\vec{\eta}_n=\mathbf{T}\cdot\vec{P}_n, \quad \vec{L}_n=2^{\vec{\eta}_n}, \tag{6}$$

where

$$\mathbf{T}=\begin{pmatrix} \alpha & 2\beta & -\alpha & \beta \\ \alpha & \beta & \alpha & -2\beta \\ \alpha & -\beta & \alpha & 2\beta \\ \alpha & -2\beta & -\alpha & -\beta \end{pmatrix}, \tag{7}$$

and $\alpha=1/4$ and $\beta=1/10$.

The basis of the local variables is plotted in Fig. 5, showing how it can be characterized as a simple ''Taylor-series'' expansion of $\vec{\eta}_n$. These variables are believed to be the right variables to monitor the dynamics of the model, since they globally describe the configuration of the local shells instead of focusing on the individual neighboring shells. The local scaling of shell models was studied earlier [9,8], but this is an instantaneous local scaling averaged over all shells and using a coarse-grained time resolution.

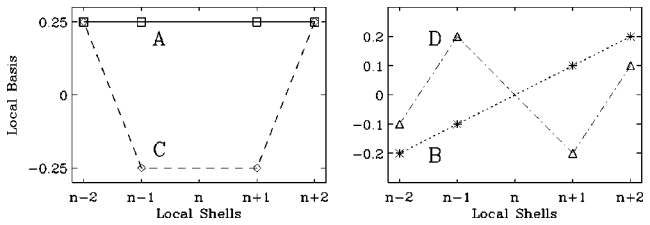

FIG. 5. The basis of the local variables, presented graphically.

A. Application to the model

To implement Eqs. (6) and (7) into the model, we assume that the components of $\vec{\eta}_n$ behave smoothly in n such that $r_n \approx 2^{A_n}$, giving

$$\dot{r}_n = -k_n 2^{2A_n}\left(2^{3B_n-D_n}-\frac{\delta}{2}2^{-2C_n}-\frac{1-\delta}{4}2^{-3B_n+D_n}\right) - \nu k_n^2 2^{A_n}. \tag{8}$$

Equation (8) gives direct evidence of the period-3 invariance of the model: Since the dynamics only depends on the combinations $(3B_n-D_n,C_n,A_n)$, we define $E_n \equiv 3B_n-D_n$. The model is then invariant to the orthogonal component of E_n: $\perp E_n=3D_n+B_n$ which is nothing but a period-3, behavior as seen in Fig. 6.

From the construction of Eq. (8) it should be noted that the sign of $\dot{r}_n$, and thereby the monotony of the dynamics, is only a function of E_n and C_n when neglecting the viscosity term. Because A_n is outside the brackets it affects the response time of the dynamics. Now the dynamics of the nth amplitude can be determined only by three local variables

$$\vec{V}_n=(E_n,C_n,A_n).$$

Even though this new set of local variables ($\vec{V}_n$) forms an efficient phase space, it should not be confused with the actual $2N$-dimensional phase space of the free variables in the model.

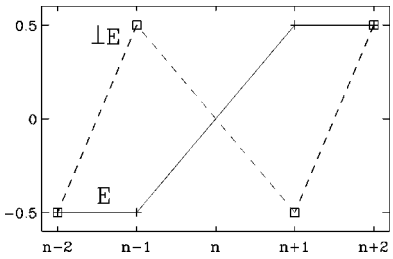

FIG. 6. Graphical presentation of $E_n,\perp E_n$, showing the period-3 invariance of the model.

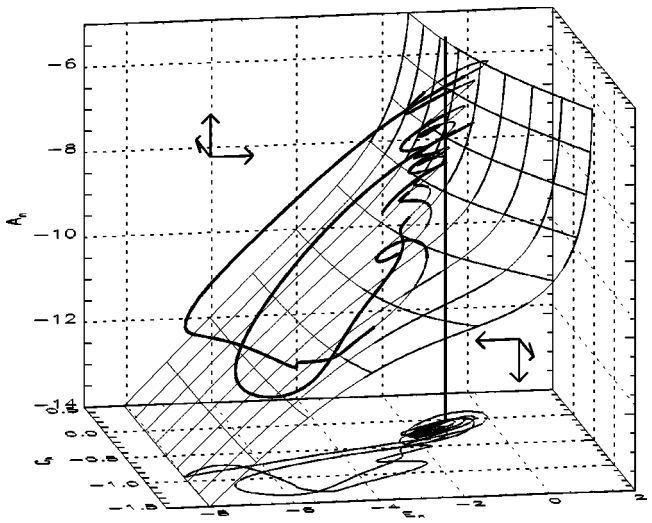

FIG. 7. The local attractor of the 14th shell and its projection on a (E_n, C_n) plane together with the surface of $\dot{r}_n = 0$, the Kolmogorov fixed-point line, and arrows of characteristic flow.

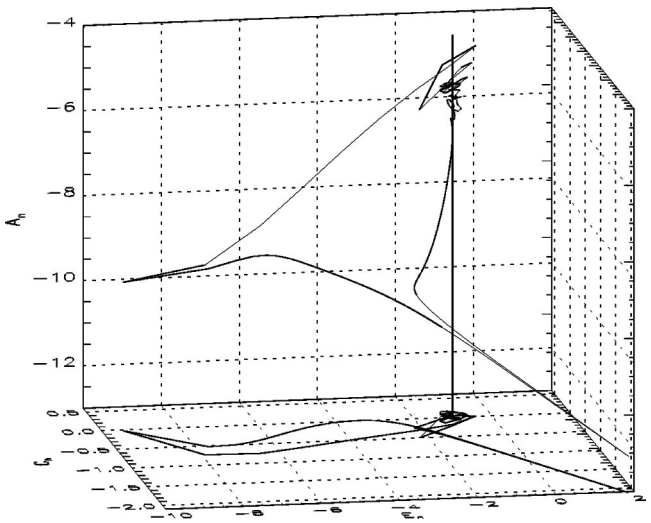

FIG. 8. The local attractor of the 14th shell for the real-valued GOY model, its projection on a (E_n, C_n) plane, and the Kolmogorov fixed-point line.

B. Local attractor of the model

Since $\vec{V}_n$ is a local phase space the trajectory of $\vec{V}_n(t)$ in time will describe a *three-dimensional local attractor* of the nth shell dynamics. Figure 7 shows the local attractor of the 14th shell during a time span of two successive bursts, where some additional features are placed to explain the dynamics of the attractor in detail.

First we note that the trajectory is projected down on an (E_n, C_n) plane to help give a three-dimensional understanding of the attractor. Then we focus on the vertical line which corresponds to the Kolmogorov fixed point given by $(E_n, C_n, A_N) = (-1, 0, \cdot)$. After every burst the trajectories encircle this line during the relaxations. As the oscillations die out the dynamics slows down, making the trajectories stay close to the region of $\dot{r}_n \approx 0$ in $\vec{V}_n$. In Fig. 7 the curved sheet is the manifold of $\dot{r}_n = 0$ derived from Eq. (8), and it is seen how the trajectory stays close to the manifold (note that the trajectory is shown thinner for negative $\dot{r}_n$).

When a burst approaches from the lower shells it affects the configuration of local shells, forcing the trajectory away from the manifold. This causes $\dot{r}_n$, and thereby r_n, to increase rapidly, making the shell participate in the burst. During the burst the trajectory approaches the Kolmogorov fixed-point line around which it begins to circle again, etc. The same behavior repeats itself throughout the evolution of the model, *making the local attractor capture all the general dynamics of the model*.

Every other shell participating in the burst has qualitatively the same local attractor with the same characteristics, and contrary to the energy spectrum of the model the local attractor is not affected by period-3 variations, since they are removed by the construction of the local variables $\vec{V}_n$. It should be noted that if the viscous term affects only the last shells, completely abandoning the inertial range, the model will still produce bursts, and in this case the oscillations will not bend off but follow the Kolmogorov fixed-point straight down until the next burst is approached.

Since the analysis of local variable is based on the real-valued GOY model [Eq. (4)], it is appropriate to check the similarities between the local attractors of the standard- and the real-valued models. Figure 8 shows the local attractor of the real-valued model together with some of the same features as for the local attractor of the complex model in Fig. 7. Comparing the two local attractors, it is seen that they share the same characteristics, both with respect to the overall shape of the local attractors and the oscillations around the Kolmogorov fixed-point line. The profound spikes seen in the local attractor of the real-valued model (Fig. 8) correspond to the amplitudes r_n crossing zero, and thus cause the related local variables to diverge momentarily. The similarities between the two local attractors justify the analysis of the standard GOY model by local variables. It should be noted that the trajectory of the real-valued local attractor is closed because of the periodicity of the dynamics.

V. CAUSE OF INTERMITTENCY

From the behavior of the local attractor it is possible to explain the intermittent shift between bursts and oscillatory relaxation, creating the intermittent behavior of the model. What is needed is answers to the following two questions: Why is the manifold of $\dot{r}_n = 0$ stable, attracting the oscillatory state into a relaxing period? What changes this stability as a burst approaches?

A. Creation of the relaxing period

To analyze the stability of the manifold we have to know the flow in the phase space $\vec{V}_n$, and this will be done by estimating $\dot{A}_n, \dot{E}_n, \dot{C}_n$. First we again assume $r_n \approx 2^{A_n}$, to obtain $\dot{r}_n \approx \ln(2) 2^{A_n} \dot{A}_n$, which will be used to estimate $\dot{A}_n$. Then we insert $\dot{A}_n$ into the transformations of Eq. (6), obtaining $\dot{E}_n$ and $\dot{C}_n$ as function of $\dot{A}_{n+j}$, $j = \{-2, -1, 1, 2\}$. To

proceed we note that because of the regular dynamics during oscillations, all the local variables for the different shells are roughly equal despite a Kolmogorov scaling of the mean values (A_n). This makes us assume the following condition between the local variables:

$$(A_{n+j},E_{n+j},C_{n+j}) \approx \left(A_n - \frac{j}{3}, E_n, C_n \right), \quad j=\{-2,-1,1,2\}. \tag{9}$$

When inserted into the different $\dot{A}_{n+j}$'s, this causes $\dot{E}_n$ and $\dot{C}_n$ to resemble $\dot{A}_n$ within prefactors in front of the coupling- and viscous terms. *As a result the monotony of $\dot{E}_n$ and $\dot{C}_n$ follows that of $\dot{A}_n$.*

Now the general flow in $\vec{V}_n$ depends only on the sign of $\dot{r}_n$, changing at the manifold and indicated by the arrows shown in Fig. 7. From the orientation of the flow and the position of the manifold the trajectory is caused to close in on the manifold and to drift slowly downward, creating a relaxing period.

B. Bursts

The stability of the manifold and thereby of the relaxing state depends critically on the condition of Eq. (9) used in the derivation above. The thing that destroys this condition is the approach of a burst from the lower shells, affecting only r_{n-2} and r_{n-1}. The manifold then loses its stability, and the state is forced into a region of strong positive $\dot{r}_n$ making the shell participate in the burst. Now, as r_n changes violently, it causes the manifold of the higher shells to become unstable, etc., and thus *the burst spreads through the shells because of a chain reaction.*

To summarize the last part of this paper, we have seen that the basic behavior of the GOY model may be captured by the dynamics of a three-dimensional attractor. This comes from expressing the dynamics of the model in a set of variables (local variables) which are based on a global description of the neighboring shell amplitudes entering the coupling terms. With these local variables the intrinsic period-3 invariance of the model naturally drops out, and the role of the Kolmogorov scaling-law solution becomes apparent as the trajectory of the local variables oscillates around it for long periods of time.

VI. CONCLUSION

In this paper the standard GOY shell model has been analyzed on the basis of its dynamics rather than its statistics. A detailed analysis of the time evolution reveals the following.

The dynamics of the model follows two different states where violent bursts are interchanged with an oscillatory relaxing state. It is shown that the dynamics of the shells are mutually correlated, and that the bursts travel through the shells like a front. Because bursts in the model cascade nearly unaffected through the shells in the inertial range, each set of neighboring shells entering the coupling terms can be seen as local phase spaces of the corresponding shells, and when expressed in a simple ''Taylor series'' base their dynamics describes an approximate attractor of the model.

With the analysis of local variables and the resulting local attractor of the GOY model, it is shown that the intermittent behavior of the GOY model can be fully explained from a dynamical-system point of view.

ACKNOWLEDGMENTS

I would like to thank the following people for fruitful discussions concerning this work: Ken Haste Andersen, Jacob Sparre Andersen, Tomas Bohr, Jesper Borg, Paolo Muratore Ginanneschi, Martin van Hecke, Anders Johansen, Jens Juul Rasmussen, Bjarne Stenum, and my supervisor Mogens Høgh Jensen.

[1] U. Frisch, *Turbulence: The legacy of A. N. Kolmogorov* (Cambridge University Press, Cambridge, England, 1995).
[2] A.N. Kolmogorov, C. R. Acad. Sci. URSS **30**, 301 (1941); **32**, 16 (1941).
[3] F. Belin, J. Maurer, P. Tabeling, and H. Willaime, J. Phys. II **6**, 1 (1996).
[4] E. B. Gledzer, Dokl. Akad. Nauk. SSSR **209**, 1046 (1973) [Sov. Phys. Dokl. **18**, 216 (1973)].
[5] M. Yamada and K. Ohkitani, J. Phys. Soc. Jpn. **56**, 4210 (1987); Prog. Theor. Phys. **79**, 1265 (1988).
[6] M.H. Jensen, G. Paladin, and A. Vulpiani, Phys. Rev. A **43**, 798 (1991).
[7] L. Kadano, D. Lohse, J. Wang, and R. Benzi, Phys. Fluids **7**, 617 (1995).
[8] T. Bohr, M. H. Jensen, G. Paladin, and A. Vulpiani, *Dynamical system Approach to Turbulence* (Cambridge University Press, Cambridge, England, 1998).
[9] L. Biferale, A. Lambert, R. Lima, and G. Paladin, Physica D **80**, 105 (1995).
[10] R. Benzi, L. Biferale, and G. Parisi, Physica D **65**, 163 (1993).
[11] T. Dombre and J.-L. Gilson, Physica D **111**, 265 (1998).
[12] F. Okkels, Master's thesis, CATS, University of Copenhagen, Denmark, 1997 (unpublished); F. Okkels and M.H. Jensen, Phys. Rev. E **57**, 6643 (1998).
[13] O. Gat, I. Procaccia, and R. Zeitak, Phys. Rev. E **51**, 1148 (1995).